Ultraviolet continua of helium molecules

Peter C. Hill
1 Hope Street, Dickson, Canberra, Australian Capital Territory, Australia
(Received 12 December 1988)

The many bands and continua of helium are reviewed, categorizing them by wavelength. Excited helium clusters dissociate, producing ultraviolet light. The population mechanisms of these molecules are deduced by using spectra, potentials, and the time evolution of excited atoms and molecules. Quartet ion recombination is proposed as accounting for the second decay component in low-energy afterglows. The roles of He_2^+ and helium clusters are identified. Data available in the literature are used to calculate a lifetime of 0.55 nsec for the "metastable" state $A\ ^1\Sigma_u^+$ at 700 Torr. This lifetime gives a theoretical upper limit for the cross section for stimulated emission of 9×10^{-18} cm^2. The feasibility of a helium dimer laser that operates at 825 Å is assessed.

I. INTRODUCTION

During the 1920s and 1930s, ultraviolet bands and continua were discovered in helium discharges. In 1924, Lyman discovered a band at 600 Å and later Hopfield found a series of weaker bands at longer wavelengths associated with this band. Then, in 1929 Hopfield discovered a continuum[1,2] (1000–600 Å) that was later to be named after him. This ultraviolet light is generated by the photodissociation of molecular helium. Variation of pressure, temperature, and discharge method results in a wide variety of spectra (Fig. 1). Such variability is indicative of the complex decay channels, which are the subject of this work.

Historically, three factors have motivated research into these continua: (1) the helium discharge lamp is a cheap and compact source of vacuum ultraviolet (VUV) radiation, (2) information yielded about He_2 can be used to test molecular theories, and (3) He_2 plays an important role in the discharge kinetics of excimer lasers in which helium is employed as a buffer gas. In the future, it may be possible to build a helium dimer laser that will generate coherent radiation[3] at wavelengths inside the Hopfield continuum. Similar dimer lasers have already been developed for the heavier noble gases[4,5] but at longer wavelengths.

Proton-excited discharges, pulsed discharges, and dc discharges all produce distinct spectra that originate from different mechanisms. This work reviews the current understanding of these reaction mechanisms and proposes new mechanisms in the light of recent data and discoveries. Sections II–V provide an analysis of the main types of helium continua and bands, categorizing them by wavelength. From the insights obtained about the origins of these spectra regions, molecular lifetimes are reduced in Sec. VI and are used to comment on the feasibility of a helium dimer laser in Sec. VII.

II. 600-Å BAND

A pulsed beam of 4-MeV protons fired into helium at 100 Torr produces an afterglow (spectrum *A* in Fig. 1).[6]

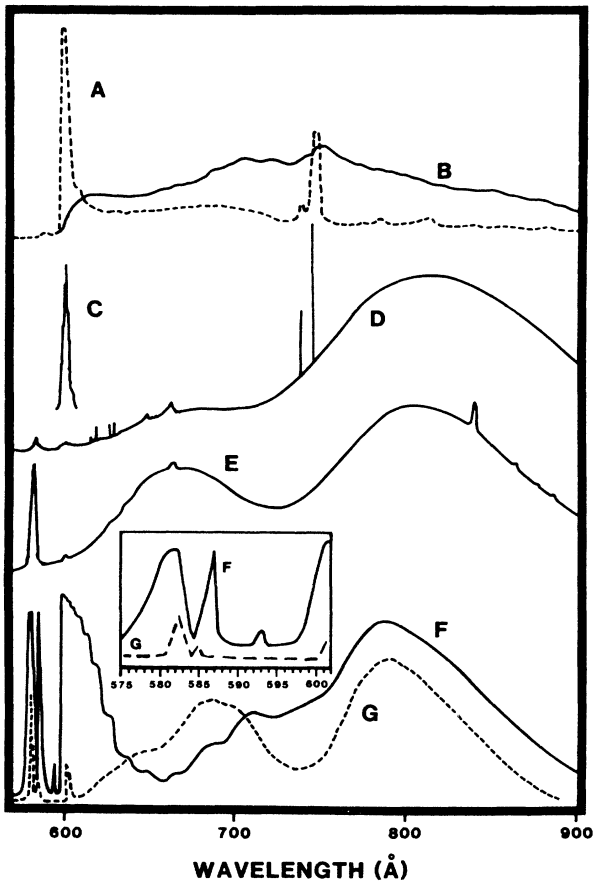

FIG. 1. Helium continua: *A*, 100 Torr, proton excited (Ref. 6); *B*, 600 Torr, proton excited (Ref. 6); *C*, 77 K, molecular beam (Ref. 3); *D*, 45 Torr, pulsed (Hopfield) (Ref. 60). *E*, 24 Torr pulsed (Hopfield) (Ref. 61); *F*, ac with no charging capacitor ("uncondensed") (Ref. 26); *G*, ac with charging capacitor ("condensed") (Ref. 26). Spectra *F* and *G* are from photographs and have a nonlinear intensity scale. This figure was created by digitizing original figures found in the references.

Molecular-beam discharges[3] (spectrum C in Fig. 1) and low-energy 3 mA dc discharges[7] produce similar spectra.

The reaction mechanisms responsible for spectrum A are detailed in this section. The excited molecules that photodissociate to generate this distribution of radiation are identified, then the reactions that form these molecules are discussed. It is proposed that two reaction mechanism be required to describe adequately the formation of the excited molecules: association (proposed by Mies and Laslett Smith[8] and recombination of quartet ions (proposed in this paper).

Proton-beam excitation is unique among methods of excitation because only a low power (a fraction of a watt) is deposited in the helium. Further, the initial composition and energy of excited helium have been calculated;[6] this has not been done for other sources. In contrast with conventional lamps discussed in later sections, the gas remains at room temperature and the concentration of products is small.

The proton-excited spectrum results from the decay of the highest vibrational levels, $v=16,17$ (Ref. 9) in $A\ ^1\Sigma_u^+$ to the ground state $X\ ^1\Sigma_g^+$. This transition obeys the selection rule ungerade $(u)\leftrightarrow$gerade (g).[10] Solution of the Schrödinger wave equation for these high vibrational levels shows that the molecule has a high expectation value at the extremes of the potential. The peak at 600 Å originates from the extended molecule, while the small internuclear separation extreme is smeared over a large range of wavelengths by the steep nature of the ground-state potential at small separations. There is little vibrational relaxation as there is no significant radiation from the lower vibrational levels. The peaks seen near 750 Å in this spectrum are generated by neon impurities.[11]

Although the molecular levels generating this spectrum are known, the time evolution of the radiation indicates that there are several processes involved in their formation. This time evolution is illustrated in Fig. 2. Bartell *et al.*[6] identified three components: first, second, and fast. In the following parts of this section the processes behind each will be deduced.

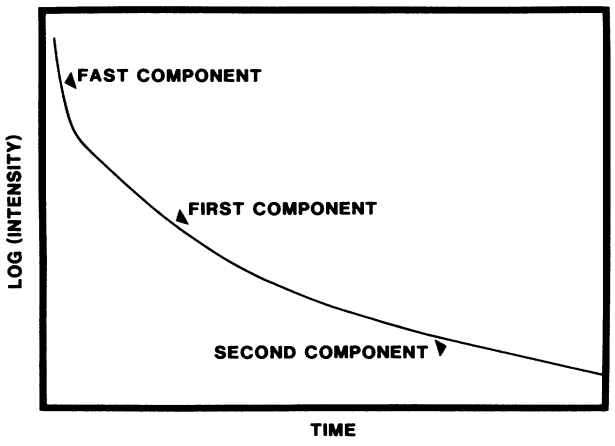

FIG. 2. Time evolution of a proton-excited afterglow, showing fast, first (association), and second (quartet-ion recombination) regions.

A. First component—association process

Bartell *et al.*[6] have identified a process that will generate this proton-excited spectrum: three-body association—

$$\mathrm{He}(2\ ^1S)+2\mathrm{He}\xrightarrow{\text{slow}}\mathrm{He}+\mathrm{He}_2(A\ ^1\Sigma_u^+, v=\max)\xrightarrow{\text{fast}}3\mathrm{He}+h\nu_{600\text{-Å band}}\ . \tag{1}$$

The $A\ ^1\Sigma_u^+$ molecule has a potential barrier of maximum height of 0.05 eV at an internuclear separation of 3.1 Å.[9] The Maxwellian distribution of velocities v,

$$P(v)=4\pi\left[\frac{m}{2\pi kT}\right]^{3/2}v^2\exp\left[\frac{-mv^2}{2kT}\right], \tag{2}$$

indicates that at room temperature ($kT=0.025$ eV) 34% of atomic collisions have sufficient energy to form this molecule. While the molecule is in a continuum state, with an internuclear separation less than 3.1 Å, a further collision with a neutral atom may cause the molecule to relax into a bound state.

Equation (1) indicates that there should be a relationship between the population of the $2\ ^1S$ state and the final radiation. Since the decay rate of the $A\ ^1\Sigma_u^+$ molecule (~ 0.55 nsec for $v=0$ at 700 Torr—see Sec. VI) is much faster than the formation rate [$\sim 30\,000$ nsec at 100 Torr—Eqs. (1) and (3)] the formation of the $A\ ^1\Sigma_u^+$ dimer is the rate-limiting step in the series of reactions that produce the final radiation. If the dimer is formed by the association process, characterized by Eq. (1), then the amount of light produced is proportional to the concentration of $2\ ^1S$. Therefore it is reasonable to attribute to the associative process the component of the radiation that has the same decay rate as the $2\ ^1S$ metastable atom.

The destruction rate of the metastable $2\ ^1S$ atom, k_m, measured in the same proton-beam apparatus used to create this spectrum,[12] is

$$k_m=220P+1.4P^2\ , \tag{3}$$

where P is in units of Torr. The first-order term may be attributed to collision-induced radiative decay to the $1\ ^1S$ state. Payne *et al.*[12] suggest that the second-order pressure term corresponds with the proposed three-body association mechanism in Eq. (1).

Bartell *et al.*[6] found that the 600-Å band radiation-decay curve (after an initial spike in intensity they called the "fast component") could be fitted by the expression

$$I_v=A_1\exp(-k_1t)+A_2\exp(-k_2t)\ . \tag{4}$$

The first and second terms of this equation refer to the first and second components of the radiation, respectively. For the radiation measured at 601 Å,[6] the pressure dependence of k_1 may be approximated by

$$k_1=6380+382P+1.09P^2\ . \tag{5}$$

The similarity between the destruction rate for the metastable atom [Eq. (3)] and for the $A\ ^1\Sigma_u^+$ molecule [Eq. (5)], as illustrated in Fig. 3, and the favorable kinetics of the association reaction at room temperature, are

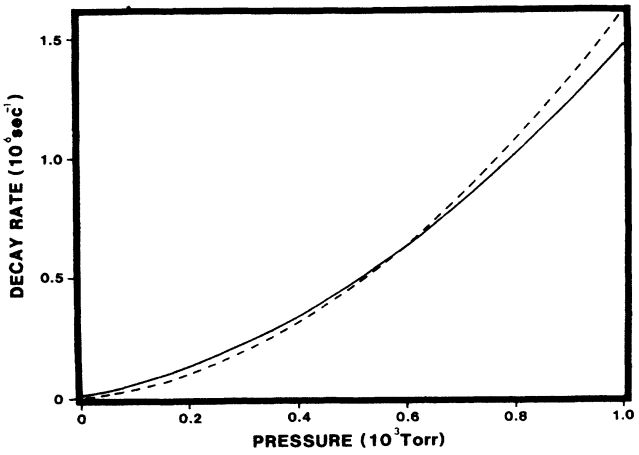

FIG. 3. Pressure dependence of the decay rate of $2\,^1S$ measured by Payne *et al.* (Ref. 12) (dashed) and of the first component of the decay rate of the $A\,^1\Sigma_u^+$ dimer as determined from data in Bartell *et al.* (Ref. 6) (solid).

compelling evidence that the reaction mechanism for the first component is association. The small discrepancy between the pressure dependence of the formation rate [Eq. (3)] and of the radiation rate [Eq. (5)] may correspond to the lifetime of the $A\,^1\Sigma_u^+(v=\max)$ molecule limiting the radiation rate at higher pressures.

B. Second component—quartet-ion recombination

The second term in Eq. (4) is consistent with a separate process that also produces vibrationally excited $A\,^1\Sigma_u^+$ molecules. At pressures below 100 Torr A_2, the coefficient of the second process, is greater than A_1. This indicates that the second process a significant source of $A\,^1\Sigma_u^+$ molecules at low pressures. The decay rate of the second process, k_2, displays no pressure dependence but shows a strong sensitivity to the initial energy of the electron-ion pairs created by the proton beam. For instance, when the initial energy per electron-ion pair drops from 43.8 to 40.0 eV, the decay rate of the second process at 200 Torr increases by 80% compared with only 10% for the first.[6] This energy sensitivity of the second process is suggestive of electronic recombination, which depends on the electron temperature among other factors.

The association process does not provide a plausible explanation of the formation of this spectrum in a dc discharge struck in the expanding jet of a molecular beam with its nozzle cooled to 77 K.[3] The average energy of the atoms in this beam is $\ll 0.007$ eV. The 0.05-eV potential barrier would make the formation of the dimer by association less likely at lower temperatures, yet Baldwin *et al.* found that there is six times more radiation at 77 K than at room temperature.

This evidence suggests a second mechanism; general principles may be invoked to aid in its identification. To generate a spectrum of this shape this second mechanism must exclusively populate the high vibrational levels of $A\,^1\Sigma_u^+$ (as was the case for the association mechanism). Expressed in terms of the Franck-Condon principle, this means that the radial wave function of the parent molecule must have significant spatial overlap with the high rather than the low vibrational levels. Knowledge of the association process (Sec. II A) adds further constraints. The association process depletes the population of the $2\,^1S$ atoms, and thus this species is not involved. Other metastable and resonantly trapped atoms are too low in energy or of too short a lifetime to form the molecule directly. These considerations will be used to eliminate molecular neutrals and doublet ions as parent molecules.

A vibrationally excited $X\,^2\Sigma_u^+$ ground state of He_2^+ is a potential parent molecule, but may be ruled out for these two reasons: (1) the ion does not remain in high vibrational states but instead undergoes rapid vibrational relaxation to the ground state $v=0$ (Ref. 13), recombining to become the lower vibrational states of the $A\,^1\Sigma_u^+$ molecule (as described in the Sec. V), and (2) the high vibrational states of the ion do not have sufficiently similar radial wave functions to fill the upper states of $A\,^1\Sigma_u^+$ exclusively. This is because the potentials themselves are considerably different at their respective high vibrational levels, due to the lack of a potential barrier for the ion state[14,15] such as that found with the molecular state.[9] The highest vibrational state of the ion is $v=22$ (Ref. 16) with radial extent 0.78 to >4 Å (Ref. 15), while the highest vibrational state of the molecule is $v=17$ with a radial extent of 0.73–3.1 Å.[9]

The $X\,^2\Sigma_u^+$ state is not involved in the formation of these vibrationally excited levels of the $A\,^1\Sigma_u^+$ molecule. This raises an ion deficiency problem. The elimination of the $X\,^2\Sigma_u^+$ state's role in the production of this spectrum, in conjunction with the absence of the radiation from the low vibrational levels normally produced by this state (a broad peak at 825 Å, see Sec. V), imply the absence of the $X\,^2\Sigma_u^+$ molecule. Since $X\,^2\Sigma_u^+$ is formed in the afterglows from the reaction of neutrals with atomic ions [Eq. (13)], the absence of this molecule implies the absence of the atomic ions. This is contrary to the prediction that atomic ions are a major product of these proton beams.[6] Any explanation of the second process must also account for the absence of these atomic ions.

There are no doublet states[17] observed or predicted lying above the $X\,^2\Sigma_u^+$ that are sufficiently similar to the $A\,^1\Sigma_u^+$ state to fill this vibrational level exclusively.

The metastable quartet state $X\,^4\Sigma_u^+$ was identified[18] when two separate molecular-ion drift velocities were discovered.[19] The quartet state is metastable because transition from $X\,^4\Sigma_u^+$ to $A\,^2\Sigma_g^+$ or $X\,^2\Sigma_u^+$ (the only ion states of lower energy) breaks the selection rule: quartet $\not\rightarrow$ doublet. This ion, consisting of He^+ and He $2\,^3S$, is faster than the $X\,^2\Sigma_u^+$ ion, which consists of He^+ and He $1\,^1S$, because the latter undergoes resonant collisions as it drifts through the He $1\,^1S$. This quartet state was observed to be the exclusive product of low-power, narrow-pulsewidth discharges.[19] The slower $X^2\Sigma_u^+$ could only appear if sufficient time were allowed for decay of the $X\,^4\Sigma_u^+$ state. As there is no potential barrier preventing formation of the quartet state, this dimer may be formed by simply multibody thermal collisions of ions with $2\,^3S$:

$$He + He^+ + He(2\,^3S) \rightarrow He_2^+(X^4\Sigma_u^+) + He \,. \quad (6)$$

Recombination of this quartet-ion state can produce the 100-Torr proton beam spectrum A. In the highest vibrational level this bound particle has internuclear separations ranging from 2.3 to 8.4 Å and will recombine to the high vibrational levels of the $A\,^1\Sigma_u^+$ state at radius of 2.3–3.1 Å (Fig. 4). This range of overlap explains the exclusive population of states having a large radial extent. Because the quartet ion is a product of these low-energy afterglows and recombines to produce this radiation, it merits consideration for the second process.

The metastable $2\,^3S$ atoms act as a sink for helium ions, solving the ion deficiency problem. Quartet-ion formation [Eq. (6)] competes successfully with neutral atoms that would otherwise form the ground ion $X\,^2\Sigma_u^+$ state. This is why this process is observed to the exclusion of other processes that would produce radiation from the lower vibrational levels—the Hopfield continua.

The confirmed existence of the quartet state in the afterglow, the lack of Hopfield radiation indicating the absence of the ground-state molecular ion, the overlap of the radial extents of this quartet potential with the $A\,^1\Sigma_u^+$ potential leading to the population of the observed levels, the height of the potential barrier of the $A\,^1\Sigma_u^+$ state making the association insignificant at 77 K, and the evidence of a second mechanism dependent on recombination all support the hypothesis that the second process is recombination of the quartet state.

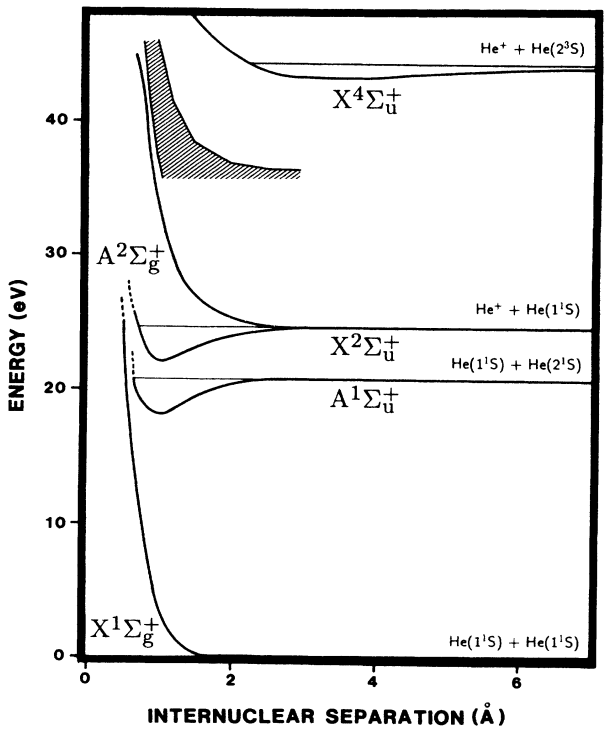

FIG. 4. Potential-energy curves of various electronic states of He_2 and He_2^+. The fine horizontal lines indicate the radial extent of the topmost vibrational levels of the various potentials. At this scale the potential barrier of the $A\,^1\Sigma_u^+$ state (0.05 eV) is not seen. The shaded region shows the possible energy and radial extent of the potential that by decaying to the $A\,^2\Sigma_g^+$ state would generate the 1050–4000-Å continuum. Source (top to bottom), Refs. 18, 14, 16, 16, and 62.

Having established association and quartet recombination as the mechanisms producing this spectrum it is possible to derive information about the lifetimes of $A\,^1\Sigma_u^+$ dimers from the pressure dependence of this spectrum. Both these mechanisms initially form $A\,^1\Sigma_u^+$ in high vibrational states. Thus the spectral distribution at 600 Torr (spectrum B in Fig. 1) showing radiation from lower vibrational levels is evidence of vibrational relaxation. The lifetime of the high vibrational levels of this molecule determines whether the state vibrationally relaxes or decays to the ground state $X\,^1\Sigma_g^+$. At 100 Torr, decay occurs before vibrational relaxation, while at 600 Torr there is relaxation before decay. This means that the decay rate of the molecule in the high vibrational states does not increase with pressure as much the vibrational relaxation rate.

C. Fast component

The fast component of the proton spectra is described by Bartell *et al.*[6] At 203 Torr the fast component has a decay rate of 7.2×10^6 sec^{-1} as opposed to 0.12×10^6 sec^{-1} for the first (associative) component—some 60 times faster. The fast component has a spectral range of 950–630 Å. This indicates that the fast radiation originates from the lower vibrational levels of $A\,^1\Sigma_u^+$ and not from the $D\,^1\Sigma_u^+$ state, as proposed by Bartell *et al.*[6] The $v=0$ level in $D\,^1\Sigma_u^+$ radiates as a smooth peak principally within a range of wavelengths from 740 to 600 Å (675 Å feature on the 24-Torr spectrum E in Fig. 1 and Ref. 20) and cannot account for the 950-Å radiation. The ratio of intensity of the fast component to the other components is constant with pressure and wavelengths from 660 to 950 Å.[6] As the explanation of Bartell *et al.* has been the only one proffered, the reaction mechanism responsible for generating the fast component of the spectra, therefore, is as yet unknown. Two hypotheses as to the origin of the fast component merit consideration: (1) the fast component results from different conditions in the early afterglow, (2) the fast component is caused by the decay of the $B\,^1\Pi_g^+$ molecule.

At the beginning of the afterglow there may be a sufficient concentration of electrons for the process of superelastic collisions to become significant. This effect was illustrated by Lawler *et al.*[21] who measured a much higher the decay rate of the $2\,^1S$ state in a pulsed electrical discharge than that found in the late afterglow of a proton-beam apparatus[12] (Fig. 5). The decay rate of the fast component coincides with the higher decay rate of the $2\,^1S$ state. It might be possible that in the fast component the $A\,^1\Sigma_u^+$ is formed by association [Eq. (1)] its decay rate reflecting the rapid decay rate of the $2\,^1S$ state, and is spectral extent speculatively explained by vibrational relaxation of the high vibrational levels (corresponding with the shorter wavelength radiation) by electrons. This hypothesis is refuted by the unperturbed level

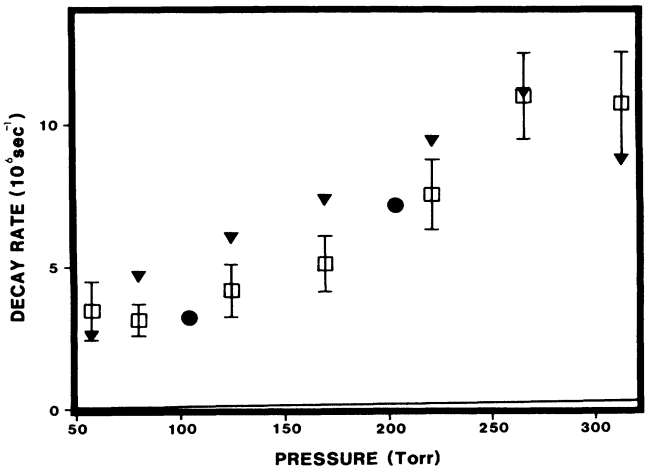

FIG. 5. Pressure dependence of decay rates: squares denote $2\,^1S$ in a pulsed discharge (Ref. 21), wedges denote $2P^3$ in a pulsed discharge (Ref. 21), and circles denote fast component of dimer decay in proton-excited helim (measured from data provided in Ref. 6). The solid curve is the decay rate of $2\,^1S$ measured in proton beam apparatus (Ref. 12) (also shown in Fig. 2).

of radiation from the higher vibrational levels during the time of the fast component. Firstly, this indicates that there is not a period of enhanced $2\,^1S$ decay, and secondly, these high vibrational levels are not destroyed by the supposed high concentration of electrons. Instead, the fast component appears to be a superaddition from a process not involving $2\,^1S$.

The $B\,^1\Pi_g^+$ state may be formed by association of neutral atoms with the $2\,^1P$ state (helium atoms). The selection rules allow this to decay the $A\,^1\Sigma_u^+$ state and thereby create the fast component. The fixed ratio of $2\,^1S$ to $2\,^1P$ created by the proton beam[6] would explain the fixed ratio of intensities of the fast and slower components.

This process also explains "prompt molecular emission" in conventional pulsed lamps described by Villarejo *et al.*[22] In the initial excitation pulse, there is emission within the same wavelength regions of the fast component. Disturbingly, as Villarejo *et al.* noted, there is insufficient time to form the $X\,^2\Sigma_u^+$ dimer ions that would normally account for this radiation (see Sec. V). Association of $2\,^1P$ atoms during the excitation pulse would provide a plausible explanation of this phenomenon.

In summary, the quartet state of the ion recombines to form the high vibrational level of the $A\,^1\Sigma_u^+$ state, which in turn decays to the ground state yielding this particular spectrum. The existence of the quartet channel in addition to the association channel accounts for a two-term decay-rate equation. The quartet channel could also explain the production of this spectrum by molecular beams in which the number of collisions and temperature would make the association unlikely on kinetic grounds. The formation of excited dimer ions by association of ions and metastable atoms may explain the absence of Hopfield continuum with this spectrum, even though atomic ions are produced by the proton beam.

III. 600–700-Å BAND SERIES AND 2100–6100-Å CONTINUUM

When the 600-Å band, discussed in the Sec. II, was investigated with high-resolution spectrometers, it was found to be the most intense and narrowest of a series of 14 or more bands stretching to longer-wavelength regions (*F* in Fig. 1). In this section, a nexus will be established between this band series and a broad continuum, the validity of which rests on the interpretation of the origins of this band series.

In the literature two explanations have been advanced for this band series: (1) the band series represents nodes in the wave function of the highest vibrational level,[7,8] and (2) the band series is the result of radiation from successive vibrational levels.[23] These explanations are not mutually exclusive.

The generation of this band series by a single vibrational level—the first hypothesis—places a number of constraints upon the position and relative intensity of these bands.

(1) The spectra must be calculable using the ground- and excited-state potentials.

(2) Since the wave functions are not affected by discharge conditions, the relative intensity of successive bands must likewise be constant under varying conditions. Minor variations may be argued for by reference to the effect of different populations of rotational levels.

(3) Since the wave function increases at the extremes of the bound potential, and the ground-state potential flattens at larger internuclear distances, the shortest-wavelength band should have the greatest intensity.

In fact, the first peak at 600 Å can be one-sixth of the intensity of the second at 601 Å.[7] This is accounted for in Sando's[9] simulation by a hybrid of the two explanations—using the two uppermost, quasibound, levels. The topmost $v=17$ level causes the 600-Å peak; this level can dissociate, explaining the weaker intensity of this peak. The $v=16$ level causes the 601-Å peak and subsequent bands result from nodes in its wave function. Sando explains the filling of these levels by free-free radiative emission.[24]

The proposition that the 600-Å band series is the result of radiation from a series of vibrational levels—the second hypothesis—was semiquantitatively described by Tanaka and Yoshino.[23] They map the position of the maxima onto the location of vibrational levels in the $A\,^1\Sigma_u^+$ state. In support of this proposition, the first seven absorption bands, which correspond to transitions of the ground state to the upper state, were found to coincide with the band peaks. The energy shifts between the emission and absorption spectra are semiquantitatively explained by consideration of the position of the maxima in the upper state in relation to the ground-state wave function of energy kT.

Perhaps the most compelling evidence that the bands between 600 and 700 Å originate from different vibrational levels is their apparent freedom from constraints (2) and (3), as shown in Table I. There is no agreement between experiment and the theoretical results. In particular, the band-to-band variability of the 20-K experimental

result (produced by an electron beam incident on superfluid helium[25]), shows no indication of being generated by the projection of a single vibrational state onto a smooth ground-state potential. Further, the absence of the first three bands may indicate that these levels are not formed at all, rather than being formed and then absorbed by the intervening gas, as was proposed by Stockton *et al.*[25] The work of Tanaka and Yoshino[23] shows that the absorption bands in this region are not sufficiently broad to block out this radiation.

The validity of the second hypothesis, that this spectrum is generated from a distribution of vibrational levels, is pivotal to an explanation of the visible continuum which is found to accompany this spectrum. If a cluster dissociates to form a $A\ ^1\Sigma_u^+$ dimer, it will fill a distribution of levels consistent with its range of internuclear separations upon fragmentation, which is likely to be different from that of a higher dimer level. Thus the generation of this spectrum from a distribution of states—hypothesis 2—is a necessary precondition for a reaction that creates this spectrum by clusters populating the $A\ ^1\Sigma_u^+$ state. Evidence for such a reaction is presented in the remaining part of this section.

In 1958 Tanaka *et al.*[26] reported the spectrum *F* seen in Fig. 1. An ac power supply for a commercial sign, with no charging capacitor (denoted as "uncondensed"), was used. This spectrum has been produced in dc discharges at room and liquid-nitrogen temperatures[7] and by bombarding superfluid helium at 20 K with electrons.[25] The band intensity in the spectrum of Tanaka *et al.* has been shown to increase with pressure up to 60 Torr.[27] The intensity of the band may still increase at higher pressures; however, this was not determined due to deterioration of discharge conditions.

The only molecular bands observed in the spectrum of Tanaka *et al.* were weak triplet bands; these are not directly involved in the singlet cascades which result in vuv radiation from the singlet $A\ ^1\Sigma_u^+$ state. Further, these bands diminished with increasing pressure, contrary to the trend of the vuv radiation. This indicates that this spectrum is not generated by the decay of higher dimer neutral and ion states to the $A\ ^1\Sigma_u^+$ state, as such transitions would produce molecular band radiation.

This lack of dimer cascade also eliminates a possible explanation of the 825-Å peak—that arises from the $v=0$ level of the $A\ ^1\Sigma_u^+$ state—found in this spectrum (see Sec. V). If dimers in higher electronic states do not decay to fill the $v=0$ level, can the top level of the $A\ ^1\Sigma_u^+$ state (formed by the processes described in Sec. II) fill the lower levels by vibrational relaxation? Examination of the 100- and 600-Torr proton-excited spectra (discussed in Sec. II B, spectra *A* and *B* in Fig. 1) reveals that the answer to this question is no. The fact that there is little vibrational relaxation in the 100-Torr spectrum renders it unlikely that there would be relaxation in the spectrum of Tanaka *et al.*'s taken at pressures between 5 and 60 Torr, the relative band intensities remaining constant over this range. Even if there were relaxation, one would expect the high vibrational levels to be depleted, as is illustrated by the absence of these levels in the 600-Torr spectra. On the contrary, in the spectrum of Tanaka *et al.*'s the highest band has the strongest intensity.

As both the cascade from higher dimer states and vibrational relaxation have been eliminated as viable explanations of the 825-Å feature, a further explanation is required. The process for the band series hypothesized in this paper also accounts for the filling of these lower vibrational levels.

The mechanism responsible for the band series is revealed by examination of an apparent by-product: a weak *continuum* stretching from the visible 6100 to $\simeq$2100 Å (Ref. 27) observed in conjunction with the 600–700-Å band series. The vuv and visible continua both increased with pressure. The 2100-Å radiation (5.9 eV) is consistent with transitions from the highest vibrational levels of molecules corresponding to atoms with large principle quantum numbers to the lowest levels in the $A\ ^1\Sigma_u^+$ state.

The existence of this continuum implies that the intermediate species is multibody, most probably He_3^*. Balasubramanian *et al.*[15] have recently treated theoretically He_3^+, an ionic species known to exist in discharges. It was determined to be the major ionic species at 82 K.[28] This cluster can be used to illustrate the process that

TABLE I. Intensity ratios of successive peaks in the 600–700 Å series (e.g., spectrum *F* in Fig. 1). The ratio of successive peaks is given in order to minimize the effects of spectrometer functions.

Peak ratios	Intensity ratios Experimental (300 K)[a]	Experimental (20 K)[b]	Theoretical (300 K)[c]
601/600	1.149	>1	0.83
602/601	0.260	>1	0.30
605/602	0.500	>1	0.30
608/605	0.577	0.76	0.50
613/608	0.626	0.92	0.51
619/613	0.723	0.56	0.61
627/619		0.79	0.57

[a]Reference 27.
[b]Reference 25.
[c]Reference 24.

leads simultaneously to this continuum and band series:

$$\begin{aligned} &He_3^+(^2\Sigma_g^+)+e\rightarrow He_2(A\,^1\Sigma_u^+)+He+h\nu_{6100-2100\ \text{Å}}\,, \\ &He_2(A\,^1\Sigma_u^+)\rightarrow He+He+h\nu_{600-1000\ \text{Å}}\,. \end{aligned} \tag{7}$$

The mean bond length of the cluster ion is 1.239 Å.[15] The Franck-Condon principle implies that this cluster would dissociate over a range of internuclear separations populating the lower vibrational levels of the dimer. The visible radiation is Hopfield-style continuum subsisting inside another—only the former contains more bodies.

IV. 1050–4000-Å CONTINUUM

Huffmann *et al.*[29] observed a broad continuum stretching from the visible to 1500 Å (8.3 eV) and thereafter rapidly reducing in intensity down to 1050 Å (11.8 eV). In their experiment a lamp was connected to a dc power supply in parallel with a capacitor which charged up to the lamp breakdown voltage and then discharged through the lamp. The continuum began at pressures of 150 Torr; although the Hopfield dimer continuum (Sec. VI) occurred with it, by about 200 Torr, the broad continuum was much stronger. The optimum operating pressure was 800 Torr. Since the repetition rate diminished with pressure the optimum pulse brightness may be at still higher pressures.

The existence of a continuum implies that some of the energy of decay is lost into fragments; therefore the species involved is multibody. The energy associated with a 1050-Å photon is too great to be that from a transition between the excited levels of the dimer (<6 eV) unlike the scenario for the 2100–6100-Å continuum in the Sec. III.

Huffman *et al.*, attributed this continuum to levels in He_2^+ on the basis of the high concentration of He^+, deduced from the broadening of He II radiation. They noted that information about the levels of He_2^+, then unavailable, would help in the identification of the likely reaction mechanism. Despite considerable progress in this area since the publication of their paper in 1960, there is still no clear explanation of this spectrum.

$X\,^2\Sigma_g^+$ states of He_2^+ have been accurately mapped using information gained from scattering experiments.[17] The $X\,^2\Sigma_u^+$ bound ground state is also accurately known.[15] It can be concluded from the value of these potentials (see Fig. 4) that the bound-bound $g\rightarrow u$ transitions are too great in energy (19 eV) to account for this radiation. A transition to the unbounded ground $A\,^2\Sigma_g^+$ (see Fig. 4) state from an excited $X\,^2\Sigma_u^+$ state could generate such a continuum. To date there are no calculations or measurements of excited $X\,^2\Sigma_u^+$ states in helium molecular ions. However, there are calculations for heavier elements, briefly reviewed by Krauss and Mies,[30] indicating that these excited $X\,^2\Sigma_u^+$ states are bound. Energy considerations dictate the radial extent of any bound state (including cluster ions) dissociating into this potential, to be within the shaded region of Fig. 4.

When Bogdanova *et al.*[31] bombarded helium impregnated metal with electrons they discovered He_2^{+*} ions of lifetime at zero pressure of 170±20 nsec. Although they calculated the ion's formation energy to be 44±2 eV, this result must be questioned as the energy of the decay products—an ion (24.59 eV) and a $3\,^3D$ (23.0 eV) or a $4\,^3D$ atom—is greater than 46 eV. The decay to these triplet atomic states indicates that the ion is a quartet state lying above and perhaps crossing the quartet potentials that dissociate to these triplet atoms. Being a quartet state it can only decay to the ground quartet state (Sec. II B) and thus could not generate this spectrum. This analysis is consistent with the failure to observe this continuum in their experiment.

He_2^{2+} appears to be an alternative explanation of this spectrum. The high density of He II radiation signifies the high densities of the double ions. The ground state of He_2^{2+} is bound between approximately 0.5 and 1.0 Å and could not produce such a continua.[17] Yagisawa *et al.*[32] have calculated the first 11 excited states of He_2^{2+}, none of which is capable of generating this radiation.

Trimer and heavier cluster ions are also possible candidates. At room temperature and 800 Torr, 4% of cluster ions are trimers. This percentage, proportional to pressure, is an extrapolation from work by Gusinov *et al.*[33] Information about He_3^{+*} and ungerade He_2^{+*} would help in the identification of a likely reaction mechanism.

Note added in proof. Blint[34] has calculated $^2\Sigma_u^+$ potentials for He_2^+. The first excited $^2\Sigma_u^+$ state has its first vibrational level at an energy of approximately 48 eV with a radial extent consistent with the shaded region of Fig. 4. I am presently attempting to confirm whether or not this molecule produces this spectrum on decay to the $A\,^2\Sigma_g^+$ state by simulating the spectrum.

V. 600–1000-Å HOPFIELD CONTINUUM

A pulsed discharge is the mostly widely used method of producing the Hopfield continuum (*D*, *E*, and *G* in Fig. 1). It attains a claimed 1% efficiency in converting electric energy to vuv light in the afterglow (700 Torr, 15 keV, 20 ka, 10-nsec pulse).[35] This high efficiency makes this process a prime candidate for a vuv dimer laser. In this section the important states and mechanisms involved in the formation of the spectrum are reviewed and the contribution of metastable states discussed.

A. Photodissociating molecules

The Hopfield continuum is caused by the decay of the first four vibrational states of $A\,^1\Sigma_u^+$ and $D\,^1\Sigma_u^+$ to the ground state $X\,^1\Sigma_g^+$.[20] The contribution of the $D\,^1\Sigma_u^+$ decreases steadily with pressure until by 100 Torr it is not observed. The relative populations of the vibrational levels are to high in energy to be thermal; rather they are the result of the recombination of molecular ions.

B. Molecular ions

To analyze the lifetime of the dimers and to achieve efficient light sources it is important to understand the process leading to the formation of these radiating states. The sequence of events occurring in the afterglow is formation of $He_2^+X\,^2\Sigma_u^+$, vibrational relaxation to the $v=0$ level, recombination, and then cascade to the $A\,^1\Sigma_u^+$ and

$D\ ^1\Sigma_u^+$ states. The molecular ion may be formed by a number of processes, including the association of neutral atoms with excited atoms, and the association of neutral atoms with ions.

If an excited helium atom has a principle quantum number $n > 3$ then the reaction, known as the Hornbeck-Molnar[36] process is exothermic:

$$He^* + He \rightarrow He_2^*(v = n) . \quad (8)$$

This reaction involves the crossing of the potential involving the excited atom with the $X\ ^2\Sigma_u^+$ (Ref. 37) ion potential leaving the ion in the vibrational level of the crossing. Its subsequent relaxation [Eqs. (10) and (11)] accounts for the extremely large atomic cross sections for this process; the $3\ ^3D$ state, for instance, has a cross section of 1.4×10^{-15} cm^2.[38]

Multibody formation by direct combination of a helium ion with ground-state atoms has been investigated by Russell:[39]

$$He^+ + He + He \rightarrow He_3^+ \rightarrow He_2^+[X\ ^2\Sigma_u^+, (v = \max)] + He . \quad (9)$$

This process has been measured by observing the change in ion-drift velocity upon the formation of the molecular ion. The reaction has been established as the major method of molecular ion production.[40] This reaction is three body, proceeding twice as fast at liquid-nitrogen temperatures as at room temperature and has a measured rate of $\kappa = 1.10(t/300)^{-0.38}\times10^{-31}$ cm^6 sec^{-1}.[39] The crucial aspect of this reaction is that it does not generate any ultraviolet light in the hot plasma conditions of an ordinary dc discharge; for this it is necessary to use the afterglow of a pulsed discharge. At some step, the series of reactions that generate the excited dimer breaks down, eliminating the radiation. The dimer itself can survive to radiate in the hot plasma, as evidenced by the prompt molecular emission discussed in Sec. II C.

Once He_2^+ is formed it rapidly relaxes to the $v = 0$ level. This is facilitated by the overlap of this potential with a large number of molecular potentials[13] allowing a cycle of autoionization

$$He_2^*(v = n) \rightarrow He_2^+(v = n - 1) + e \quad (10)$$

and recombination

$$He_2^+(v = n - 1) + e + e \rightarrow He_2^*(v = n - 1) + e \quad (11)$$

to proceed. The electron remains in a high Rydberg state and can be autoionized by a vibrational quantum, resulting in rapid vibrational relaxation of He_2^+. The ion's vibrational relaxation rates have been measured to be five times faster than gas collisions, which also relax the molecule. As recombination and the cascade to the radiating states contain the rate-limiting step, this process will be dealt with in Sec. VI.

C. Role of metastable atoms and molecules

Metastable atoms are important in determining the kinetics of the afterglow; they can modify the electron-energy distribution by superelastic collisions.[41] They can form dimers through neutral collisions and can generate ions through metastable-metastable–atom collisions. Further, they can react with atomic ions to form excited dimer ions (Sec. II). Finally, metastable atoms themselves may be formed by the dissociation of dimers and dimer ions. With so many potential reactions, interpretation of the time evolution of metastable-atom populations is difficult. The significant factor in this discussion of metastable atoms is the extent to which they couple to the final radiation. Radiation trapping adds further complexity owing to the fact that it enhances the population of resonant states so that they also appear to have metastable lifetimes.

Section II B illustrated a reaction in which metastable $2\ ^1S$ molecules reacted with neutral atoms. Another example involving $2\ ^3S$ (Ref. 42) is

$$He(2\ ^3S) + n\,He \rightarrow He_2(a\ ^3\Sigma_u^+) + (n - 1)He . \quad (12)$$

This forms an ungerade dimer which is precluded from radiating to the ground state by its parity. Even though this reaction is in strong reverse equilibrium, reaction of the product with impurities or metastable-metastable–atom collisions [Eq. (14)] serves as a sink for $He(2\ ^3S)$ and may explain the decay rate of $He(2\ ^3S)$ observed by Horiguchi *et al.*[43] The height of the potential barrier for this reaction has been calculated to be 0.08 eV.[16]

The populations of $2\ ^1S$ and $2\ ^3S$ are coupled in conditions of high electron density by a weak spin-exchange reaction discovered by Phelps[44],

$$He(2\ ^1S) + e \rightarrow He(2\ ^2S) + e , \quad (13)$$

who determined its rate to be 3.5×10^{-7} cm^3 sec^{-1}.

Metastable-metastable–atom reactions,

$$He^* + He^* + n\,He \rightarrow He^+ + n\,He + e , \quad (14)$$

have been found by Biondi[45] to have a rate of 4×10^{-9} cm^3 sec^{-1}. Such reactions are important as they couple the metastable-atom population to species that eventually create the Hopfield radiation, and also provide an explanation for the decay of $a\ ^3\Sigma_u^+$.[46] In low-pressure discharges[48] the electron population almost doubles after the termination of the pulse due to this mechanism. Hirabayashi *et al.* deduce an increase by a factor of 12 in electron population.[47] Trace impurities are found to be critical to the rate of metastable-atom conversion.

The formation of metastable atoms may be achieved by one of two processes. (1) Metastable atoms from excited atoms: Collisional-radiative recombination theory describes the atomic recombination and the Saha-Boltzmann equation[47] in the radiative regime[48] describes the cascade to the metastable atom. (2) Metastable atoms from excited dimers: this process becomes significant at higher pressures.

An important result from the analysis of the first process is that in the afterglow the electron temperature rapidly falls to the ambient temperature of the gas.[48] Controlling the operating temperature of the lamp will determine the electron-energy distribution in afterglows.

The second process constitutes a significant dimer loss channel. Generation of excited helium atoms associated with the recombination of He_2^+ has been observed.[49] The atomic 10 830-Å radiation from the $2\,^3P$ to $2\,^2S$ transition has an anomalous decay curve in that it follows that of the helium molecules. The following reaction has been proposed[50] for the generation of $2\,^3P$:

$$\begin{aligned} &He + He_2^+ \rightarrow He_3^+ , \\ &He_3^+ + e \rightarrow He(2\,^3P) + 2He , \\ &He(2\,^3P) \rightarrow He(2\,^3S) + h\nu_{10\,830\ \text{Å}} . \end{aligned} \tag{15}$$

This is one example of a class of possible reactions called Rydberg dissociative recombination, in which recombination can occur at different stages. This reaction is only feasible for He_2^* molecules with energy greater than the dissociation products.

In summary, the concentration of metastable and other species in the afterglow will determine which of many complex reaction paths will dominate, and whether the presence of metastable atoms will impede or enhance the final radiation.

VI. LIFETIMES

Any comment on the feasibility of a helium dimer laser relies upon an understanding of molecular lifetimes. Firstly, the lifetime of the upper state bears on issues within the lasing process itself, such as cross section, competing mechanisms, and laser design. Secondly, the lifetimes of processes that lead to the upper state determine which method of excitation most effectively fills this state.

The lifetime of the metastable $A\,^1\Sigma_u^+$ state at 700 Torr (Ref. 51) 0.55 nsec. This is calculated from

$$I = \frac{\delta N}{\delta t} = \kappa N , \tag{16}$$

where N is the population of $A\,^1\Sigma_u^+ = 6.1 \times 10^{11}$ cm^{-3}, κ is the rate, and the photon density is $I = 1.1 \times 10^{21}$ photons/cm^3 sec. The decay rate may be influenced by the electron and neutral density and thus may be slower at lower pressures. Measurements of the intensity and population, similar to those made by Stevefelt *et al.*,[51] are required at different pressures to determine the pressure dependence and the natural lifetime. 0.55 nsec is a lower limit of the natural lifetime of this molecule. Lifetimes for other noble gas dimers, at pressures > 100 Torr are for Ar_2, 2.9 μsec; Kr_2, 265 nsec; and Xe_2, 100 nsec.[52]

Gand *et al.*[35] show that, in the operation of a conventional pulsed source, the higher pressures achieve brighter peak intensities and thus greater population of the upper state. Consequently, the 700-Torr value of the lifetime is relevant to the operation of lasers.

For a lasing process it is critical to utilize the method that achieves a large population of the upper state. The level before the rate-limiting step in a cascade will have the largest population. Nonexponential recombination rates lead to complex evolution of populations in the afterglow radiation. To date that has been no completely successful quantitative description of this time evolution. What follows is a qualitative description.

In a high-energy pulse the high concentrations of electrons and metastable atoms lead to the reactions and the Hopfield radiation described in Sec. V. The reactions and periods described for a low-energy pulse in Sec. II are no longer appropriate. The decay curves of a high-energy pulse afterglow contain three regions: deadtime, molecular-decay limited, and recombination limited. The extents of these regions depend upon competition between mechanisms in varying discharge conditions.

There are two mechanisms of recombination: collisional

$$He_2^+ + e + e \rightarrow He_2^*(\text{low electronic states}) + e , \tag{17}$$

and radiative,

$$He_2^+ + e \rightarrow He_2^*(\text{high electronic states}) . \tag{18}$$

The two mechanisms are not distinct and are best described by a hybrid theory, "collisional-radiative recombination."[53] This theory is embodied in the experimental value for the recombination rate by Deloche *et al.*:[54]

$$\alpha_{CR} = [\alpha_c + k_1(\text{He})]\mathcal{T}^{-x} + k_2(e)\mathcal{T}^{-y} , \tag{19}$$

where α_{CR} is the rate of combination, $\alpha_c < 5 \times 10^{-10}$ cm^3 sec^{-1}, $k_1 = 5 \pm 1 \times 10^{-27}$ cm^6 sec^{-1}, $k_2 = 4.0 \pm 0.5^{-20}$ cm^6 sec^{-1}, and $\mathcal{T} = T_e/293$ K. $x = 1 \pm 1$, while $y = 4.0 \pm 0.5$.

Collisional recombination occurs more rapidly at low electron temperatures. Increasing the density of electrons will significantly increase the intensity of the initial radiation. Most importantly, collisional recombination tends to form the lower electronic states, namely, $A\,^1\Sigma_u^+$. This offers two advantages.

(1) At sufficiently high electron densities the recombination rate is faster than the intermediate states decay rate. By circumventing these slower steps a higher peak intensity and a higher population of the $A\,^1\Sigma_u^+$ state can be achieved.

(2) There are fewer losses to dissociative or other reaction channels.

When the electron density reduces, radiative recombination is the dominant reaction and the molecular ion forms higher excited states. The decay tends to take a $u \rightarrow g \rightarrow u$ path to the $A\,^1\Sigma_u^+$ state, while in these states the molecules may dissociate. In these conditions some 70% of dimers are calculated[54] to dissociate without generating the Hopfield continuum.

This path produces the molecular bands observed in the visible region. Initially, the molecular band decay rate is less than the uv radiation[51] because the molecular bands do not include radiation from the collisional path. While the recombination rate is faster than the decay rate of intermediate molecular states, the latter is the rate-limiting step. This corresponds to the intermediate decay region where the decay rate departs from the recombination rate.

Ultimately, the recombination rate will become slower than the molecular radiation rate. Once more, recombination will be the rate-limiting step.

Using data from Gand *et al.*[35] and Huffman *et al.*,[55] it may be induced that the product of the pressure and the time required to reach a maximum intensity of 800-Å light is constant over a pressure range of 44–700 Torr,

$$P\tau = 5.40 \pm 0.20 \times 10^{-5} \text{ Torr s} . \quad (20)$$

This may be interpreted as the time required for the electron-energy distribution to decrease to a point which permits molecular recombination to commence.

The significance of the recombination of the molecular ion in the production of the dimer is demonstrated by the phenomenon of dead time. Huffmann *et al.*[55] observed that at 44 Torr, regardless of intensity, there was a 20-ns dead time between the excitation pulse and the commencement of the afterglow. Observation of He $2\,^1S$ shows that at 50 Torr (Ref. 43) it monotonically decays over 20 nsec. A plausible explanation for these phenomena is as follows. At this gas pressure the He $2\,^1S$ undergoes superelastic collisions with electrons, maintaining a high electron temperature which in turn prevents the recombination of the molecular ion until the population of He $2\,^1S$ is depleted. The cross section for superelastic collision at 300 K has been measured to be 3×10^{-14} cm^2.[44]

Analysis of lifetimes is crucial to laser design. For the design involving molecular beams described by Baldwin *et al.*[3] a lifetime with the highest vibrational level of the $A\,^1\Sigma_u^+$ state of the order of milliseconds would be required for it to survive for a reasonable gain length. Considering other laser schemes, the efficiency of collisional recombination, together with the short lifetime of the dimer, heighten the importance of achieving an intense pulse with a high electron density.

VII. FEASIBILITY OF A HELIUM DIMER LASER

A population inversion between the excited states (lifetime 5×10^{-10} sec) and unbound ground state (lifetime 10^{-14} sec) makes it possible to build a helium dimer laser that will produce tunable radiation in the region of 800 Å. This region is already accessed by tripling and other four-wave sum-mixing technique using gases as a nonlinear medium. The efficiency of such conversions is at best 1×10^{-4}.[56] Free-electron lasers and optical klystrons[57] are other areas that will, in time, produce coherent light at these wavelengths.

The equation determining the gain criterion[5] is

$$\sigma_{\text{atom}} = \frac{\lambda^4}{8\pi\tau c\,\Delta\lambda} = 9\times10^{-18} \text{ cm}^2 , \quad (21)$$

where λ is the wavelength (825 Å), σ is the cross section for stimulated mission, τ is the natural lifetime (>0.55 nsec), and $\Delta\lambda$ is the width of the transition; in this case, 125 Å is on the basis of the spectrum of Gand *et al.*[35] The value 9×10^{-18} cm^2 is the maximum value of the cross section for stimulated emission. This compares favorably with the cross section for Ar_2 of 1×10^{-17} cm^2 in which laser action has been demonstrated (60 atm at 1260 Å, the end mirrors having 5% reflectivity[4]). Dimer lasers have already been achieved in argon and xenon, the major problems being radiation damage to the optics.

The cross section per molecule is inversely proportional to the lifetime τ. The population of the upper state is proportionate to τ making σ_{tot} independent of τ. Therefore, the upper-state lifetime is of secondary importance, pertaining to issues such as the bandwidth of the outcoming radiation and the susceptibility of the upper state to alternate reactions (if the molecule has a long lifetime it is likely to react). Paramount to lasing is the population of the excited state (N); the method that produces the greatest peak intensity is best suited to stimulated emission. Critical to achieving a large peak intensity is rapid recombination and direct formation of the $A\,^1\Sigma_u^+$ state found in high-pressure, high-electron-density pulsed discharges.

Mirrors at the end of the cavity will reduce the gain requirements. Tungsten has a reflectivity of 25% in this region,[58] while iridium coated with aluminum (400 Å) (Ref. 59) has a theoretical normal incidence reflectivity of 70% at 825 Å. If the reflectors also polarize the light, one example being a corner reflector, this would increase the effective gain by a factor of up to $\sqrt{2}$. Such a corner reflector can be made to focus the radiation by constructing it with two toroidal mirrors that are designed to image at a grazing angle of 45°. The mirrors are cut and joined at an angle of 90°.

Despite the apparent feasibility of this laser, there are engineering problems to overcome. Not the least of these is the fact that this wavelength of radiation is absorbed by air (as is 1260 Å).

In summary, the $A\,^1\Sigma_u^+$ state has a cross section for simulated emission comparable to other dimers in which lasing has been demonstrated. A large population of this state can be obtained in high-pressure pulsed discharge and there are high reflectivity mirrors available for the ends of the resonant cavity.

VIII. CONCLUSION

This work has identified key population mechanisms of He_2^*. Quartet-ion recombination was hypothesized to explain the time evolution of proton-excited afterglows. Various continua were linked with different processes, highlighting the role of clusters and molecular ions. The Hopfield continua were discussed in order that the feasibility of vuv laser be accessed.

Future enquires into this topic might address the nature of the potential responsible for the 1050–4000-Å continuum, the lifetime of the higher vibrational levels in the $A\,^1\Sigma_u^+$ molecule, and vibrational relaxation mechanisms. Insights into molecular physics gained and the potential commercial applications, especially lasers, would reward such investigations.

[1]J. Hopfield, Phys. Rev. **35**, 1133 (1930).
[2]J. Hopfield, Phys. Rev. **36**, 784 (1930).
[3]K. Baldwin, R. Swift, and R. Watts, Rev. Sci. Instrum. **58**, 812 (1987).
[4]W. Wrobel, H. Röhr, and K. Steur, Appl. Phys. Lett. **36**, 113 (1980).
[5]M. Hutchinson, Appl. Phys. **21**, 95 (1980).
[6]D. Bartell, G. Hurst, and E. Wagner, Phys. Rev. A **7**, 1068 (1973).
[7]A. Laslett Smith, J. Chem. Phys. **49**, 4817 (1968).
[8]F. Mies and A. Laslett Smith, J. Chem. Phys. **45**, 994 (1966).
[9]K. Sando, Mol. Phys. **23**, 413 (1972).
[10]G. Herzberg, *Molecular Spectra and Molecular Structure,* Vol. 2 of *Spectra of Diatomic Molecules,* (Van Nostrand, Princeton, NJ, 1950).
[11]R. Kelly and L. Palumbo, Naval Research Laboratory Report No. 7599, 1972.
[12]M. Payne, G. Hurst, M. Nayfeh, J. Judish, C. Chen, E. Wagner, and J. Young, Phys. Rev. Lett. **35**, 1154 (1975).
[13]J. Stevefelt, Phys. Rev. A **8**, 2507 (1973).
[14]A. Khan and K. Jordan, Chem. Phys. Lett. **128**, 368 (1986).
[15]K. Balasubramanian, M. Z. Liao, and S. H. Lin, Chem. Phys. Lett. **142**, 349 (1987).
[16]K. Sunil, J. Lin, H. Siddiqui, P. Siska, and K. Jordan, J. Chem. Phys. **78**, 6190 (1983).
[17]A. Metropoulos, C. Nicolaides, and R. Buenker, Chem. Phys. **114**, 1 (1987).
[18]E. Beaty, J. Browne, and A. Dalgarno, Phys. Rev. Lett. **16**, 723 (1966).
[19]J. Madson, H. Oskam, and L. Chanin, Phys. Rev. Lett. **15**, 1018 (1965).
[20]H. Michels, R. Hobbs, and J. Peterson, Chem. Phys. Lett. **134**, 571 (1987).
[21]J. Lawler, J. Parker, L. Anderson, and W. Fitzsimmons, Phys. Rev. Lett. **39**, 543 (1977).
[22]D. Villarejo, R. Herm, and M. Ingram, J. Opt. Soc. Am., **56**, 1574 (1966).
[23]Y. Tanaka and K. Yoshino, J. Chem. Phys. **50**, 3087 (1969).
[24]K. Sano, Mol. Phys. **21**, 439 (1971).
[25]M. Stockton, J. Keto, and W. Fitzsimmons, Phys. Rev. A **5**, 372 (1972).
[26]Y. Tanaka, A. Jursa, and F. LeBlanc, J. Opt. Soc. Am. **48**, 304 (1958).
[27]Y. Tanaka and K. Yoshino, J. Chem. Phys. **39**, 3081 (1963).
[28]C. de Vries and H. Oskam, Phys. Lett. **29A**, 299 (1969).
[29]R. Huffman, Y. Tanaka, and J. Larrabee, J. Opt. Soc. Am. **52**, 851 (1962).
[30]M. Krauss and F. Mies, *Excimer Lasers* (Springer-Verlag, Berlin, 1979), Vol. 40, Chap. 2.
[31]I. Bogdanova, V. Marusin, and V. Yakhontova, Opt. Spektrosk. **60**, 1138 (1986) [Opt. Spectrosc. (USSR) **60**, 705 (1986)].
[32]H. Yagisawa, H. Sato, and T. Watanabe, Phys. Rev. A **16**, 1352 (1977).
[33]M. Gusinow, R. Gerber, and J. Gerardo, Phys. Rev. Lett. **25**, 1248 (1970).
[34]R. Blint, Phys. Rev. A **14**, 2055 (1976).
[35]M. Gand, A. Bouchoule, and J. Stevefelt, Appl. Phys. Lett. **35**, 50 (1979).
[36]A. Hornbeck and J. Molnar, Phys. Rev. **84**, 621 (1951).
[37]J. Cohen, Phys. Rev. A **13**, 86 (1976).
[38]M. Teter, F. Niles, and W. Robertson, J. Chem. Phys. **44**, 3018 (1966).
[39]J. Russell, J. Chem. Phys. **84**, 4394 (1986).
[40]A. Phelps and S. Brown, Phys. Rev. **86**, 102 (1952).
[41]C. Gorse, J. Bertagne, and M. Capitelli, Phys. Lett. A **126**, 277 (1988).
[42]J. Pouvesle and J. Stevefelt, J. Chem. Phys. **83**, 2836 (1985).
[43]S. Horiguchi, M. Saito, K. Nakamura, and T. Nakaya, Opt. Commun. **60**, 383 (1986).
[44]A. Phelps, Phys. Rev. **99**, 1307 (1955).
[45]M. Biondi, Phys. Rev. **82**, 453 (1951).
[46]G. Myer and A. Cunningham, J. Chem. Phys. **67**, 1942 (1977).
[47]A. Hirabayashi, Y. Nambu, M. Hasuo, and T. Fujimoto, Phys. Rev. A **37**, 77 (1988).
[48]C. Collins and W. Hurt, Phys. Rev. **167**, 166 (1967).
[49]C. Collins and W. Hurt, Phys. Rev. **179**, 203 (1969).
[50]D. Bates, J. Phys. B **17**, 2363 (1984).
[51]J. Stevefelt, J. Pouvesle, and A. Bouchoule, J. Chem. Phys. **76**, 4006 (1982).
[52]B. Stoicheff, *Frontiers of Laser Spectroscopy of Gases,* edited by A. Alves, J. Brown, and J. Hollas (Kluwer Academic, Dordrecht, 1988), p. 63.
[53]D. Bates, A. Kingston, and R. McWhiter, Proc. R. Soc. London **267**, 297 (1962).
[54]R. Deloche, P. Monochicourt, M. Cheret, and F. Lambert, Phys. Rev. A **13**, 1140 (1976).
[55]E. Huffmann, J. Larrabee, Y. Tanaka, and D. Chambers, J. Opt. Soc. Am. **55**, 101 (1965).
[56]G. Hilber, A. Lago, and R. Wallenstein, J. Opt. Soc. Am. B **4**, 1753 (1987).
[57]J. Ortega, Y. Lapierre, B. Girard, M. Billardon, P. Elleaume, C. Bazin, M. Bergher, M. Velge, and Y. Petroff, IEEE J. Quantum Electron. **QE-21**, 909 (1985).
[58]I. Sobel'man and V. Vinagradov, *Advances in Atomic and Molecular Physics: On the Problem of Extreme UV and X-ray Lasers* (Academic, New York, 1985), Vol. 20, p. 327.
[59]G. Hass and W. Hunter, Appl. Opt. **6**, 2097 (1967).
[60]R. Huffmann, J. Larrabee, and D. Chambers, Appl. Opt. **4**, 1145 (1965).
[61]W. Lindermann, Ph.D. thesis, Adelaide University, 1982.
[62]F. Van Duijneveldt, Chem. Phys. Lett. **143**, 435 (1968).